



# 基于冠状动脉CT血管成像的力学组学预测心肌桥近端斑块形成

陈艳春<sup>1</sup>, 郑金<sup>2,3</sup>, 滕忠照<sup>3,4△</sup>, 张龙江<sup>1△</sup>

1. 南京医科大学金陵临床医学院/东部战区总医院 放射诊断科(南京 210002);

2. 帝国理工学院 医学研究委员会 医学科学实验室(伦敦 SW7 2AZ);

3. 剑桥大学医学院 放射系(剑桥 CB2 0QQ); 4. 南京景三医疗科技有限公司(南京 210002)

**【摘要】目的** 利用机器学习的方法评估基于冠状动脉CT血管成像(coronary CT angiography, CCTA)的力学组学对左冠状动脉前降支心肌桥近端斑块形成的预测价值。**方法** 回顾性搜集2007年1月-2021年4月在我院行至少2次CCTA检查示左冠状动脉前降支心肌桥且基线左冠状动脉前降支无粥样硬化斑块的患者,两次CCTA检查间隔3个月以上。心肌桥近端粥样硬化斑块的形成为主要终点事件。记录患者的人口学特征和临床危险因素并将不同组别患者按照年龄性别进行1:1匹配。基于CCTA进行计算流体动力学分析。在CCTA图像上测量心肌桥的位置、长度、深度和收缩期狭窄指数,以及提取左冠状动脉前降支近段的力学组学参数。利用多因素Cox回归筛选有意义特征,采用随机森林算法挑选力学组学特征并进行后续建模,为每个患者的力学组学特征进行赋值评分。采用对数秩检验方法和Kaplan-Meier图探讨力学组学模型对未来斑块形成的预测价值。采用受试者工作特征曲线评估不同心肌桥组对斑块形成的预测价值。**结果** 该研究共纳入104例左冠状动脉前降支心肌桥患者,其中52例患者心肌桥近端斑块形成,中位随访时间为3.0年。总人群的平均年龄为(54.56±10.56)岁,75.00%(78/104)为男性。除吸烟史外(21.15% vs. 5.77%,  $P=0.04$ ),其余的临床及解剖学特征在有无斑块形成组间差异无统计学意义(所有 $P>0.05$ )。入组患者按照7:3分为训练集( $n=74$ )和验证集( $n=30$ ),随机森林算法构建的力学组学模型按照赋分 $\geq 0.46$ 和 $<0.46$ 为赋分较高组和赋分较低组,力学组学模型在验证组的敏感性、准确性分别为0.87(0.58~0.98)和0.63(0.44~0.79)。多因素Cox回归模型中,力学组学(危险比=10.58;95%置信区间:3.23~34.64,  $P\leq 0.001$ )与斑块形成呈正相关。通过对数秩检验力学组学赋分较高组相对于赋分较低组在心肌桥近端更容易形成斑块( $P<0.001$ )。全部人群、训练集、验证集、表浅心肌桥组、长心肌桥组和短心肌桥组力学组学预测斑块形成曲线下面积分别为0.88(0.82~0.95)、0.89(0.82~0.96)、0.86(0.74~0.99)、0.92(0.86~0.97)、0.86(0.74~0.98)和0.91(0.83~0.98)。**结论** 力学组学对左冠状动脉前降支心肌桥近端动脉粥样硬化斑块形成有一定预测价值。

**【关键词】** 冠状动脉CT血管成像 心肌桥 力学组学 斑块形成 机器学习

**Coronary CT Angiography-Based Mechanomics Predicts Atherosclerotic Plaque Formation in Regions Proximal to Myocardial Bridging** CHEN Yanchun<sup>1</sup>, ZHENG Jin<sup>2,3</sup>, TENG Zhongzhao<sup>3,4△</sup>, ZHANG Longjiang<sup>1△</sup>. 1. Department of Diagnostic Radiology, Jinling Hospital/General Hospital of Eastern Theater Command of PLA, Nanjing Medical University, Nanjing 210002, China; 2. MRC Laboratory of Medical Sciences, Imperial College London, London SW7 2AZ, United Kingdom; 3. Department of Radiology, School of Clinical Medicine, University of Cambridge, Cambridge CB2 0QQ, United Kingdom; 4. Nanjing Jingsan Medical Science and Technology, Ltd., Nanjing 210002, China

△ Corresponding author, TENG Zhongzhao, E-mail: [zt@tenoke.com](mailto:zt@tenoke.com); ZHANG Longjiang, E-mail: [kevinzhjl@163.com](mailto:kevinzhjl@163.com)

**【Abstract】 Objective** To assess with machine learning the predictive value of mechanomics derived from coronary CT angiography (CCTA) for atherosclerotic plaque formation in regions proximal to myocardial bridging (MB) in the left anterior descending coronary artery (LAD). **Methods** This retrospective study included a cohort of patients with MB in LAD and no atherosclerotic plaque formation in LAD as confirmed by two CCTA conducted between January 2007 and April 2021 at our hospital. The interval between the two CCTA examinations was more than 3 months. The primary endpoint was the formation of atherosclerotic plaques in regions proximal to the myocardial bridging. Patient demographic characteristics and clinical risk factors were documented. Then, the patients were matched by age and sex in a 1-to-1 ratio and divided into two groups, those with plaque formation and those without plaque formation. Computational fluid dynamics analysis was performed based on CCTA. Key anatomical parameters of MB, including location, length, depth, and systolic compression index, were meticulously measured on the CCTA images. Mechanomic data were extracted from the region proximal to the MB. A multivariate Cox regression analysis was performed to identify significant features. A random forest algorithm was used to select mechanomic features for subsequent modeling and to assign scores for each patient's mechanomic features. The log-rank test and Kaplan-Meier curves were used to investigate the mechanomic model's predictive performance concerning plaque formation. Additionally, the operator characteristic

△ 通信作者,滕忠照, E-mail: [zt@tenoke.com](mailto:zt@tenoke.com); 张龙江, E-mail: [kevinzhjl@163.com](mailto:kevinzhjl@163.com)

curves were applied to evaluate how well the model could predict plaque formation across various myocardial bridge subgroups. **Results** A total of 104 patients with LAD MB were recruited. The mean age of the subjects were ( $54.56 \pm 10.56$ ) years and 75.00% (78/104) of them were male. Among them, 52 developed plaque formation over a median follow-up period of 3.0 years. Apart from a smoking history, which was more prevalent in the group with plaque formation than that in the group without plaque formation (21.15% vs. 5.77%,  $P=0.04$ ), no significant differences between the groups were observed in terms of the other clinical or anatomical characteristics (all  $P \leq 0.05$ ). The participants were divided into a training set ( $n=74$ ) and a validation set ( $n=30$ ) at a 7 : 3 ratio. With the mechanics model constructed using the random forest algorithm, the patients were classified into a high-score group ( $\geq 0.46$ ) and a low-score group ( $< 0.46$ ) based on a cutoff score of 0.46. The mechanics model achieved a sensitivity of 0.87 (0.58-0.98) and an accuracy of 0.63 (0.44-0.79) in the validation set. The multivariate Cox regression model revealed a strong positive association between mechanics and plaque formation (hazards ratio [HR]: 10.58; 95% confidence interval [CI]: 3.23-34.64,  $P < 0.001$ ). The log-rank test showed that the high-score group in the mechanics model was more likely to develop plaques at the proximal regions of the myocardial bridge compared to the low-score group ( $P < 0.001$ ). The area under the curve (AUC) for plaque formation, as predicted by the model, was 0.88 (95% CI: 0.82-0.95) for the entire population, 0.89 (95% CI: 0.82-0.96) for the training set, 0.86 (95% CI: 0.74-0.99) for the validation set, 0.92 (95% CI: 0.86-0.97) for the superficial MB group, 0.86 (95% CI: 0.74-0.98) for the long MB group, and 0.91 (95% CI: 0.83-0.98) for the short MB group. **Conclusion** The mechanomic assessment holds substantial potential as a predictive tool for atherosclerotic plaque formation in regions proximal to MB in LAD.

**【Key words】** Coronary CT angiography Myocardial bridge Mechanics Plaque formation  
Machine learning

冠状动脉疾病是全球主要的死亡原因之一<sup>[1]</sup>。动脉粥样硬化斑块可在冠状动脉管腔中形成局部狭窄,导致局部缺血和冠心病<sup>[2-3]</sup>。心肌桥是一种先天性冠状动脉走行异常,表现为心外膜冠状动脉节段性走行于心肌内。最常见于左冠状动脉前降支,可根据长度、深度及位置对其进行分类<sup>[4]</sup>,不同检查方式及队列报告的心肌桥的患病率差异很大<sup>[5]</sup>,基于冠状动脉CT血管成像(coronary CT angiography, CCTA)的研究报道了在普通人群中心肌桥的患病率约为30%<sup>[6]</sup>。虽然大多数心肌桥是良性的,但心肌桥在收缩期短暂压迫冠状动脉管腔,血流量仅为正常的15%,这一过程被称为动态狭窄<sup>[5,7]</sup>,可能会导致血流动力学异常并引起稳定型心绞痛、心肌缺血、室性心动过速甚至心源性猝死<sup>[8-10]</sup>。此外,心肌桥近端容易出现动脉粥样硬化,而壁冠状动脉段相对没有<sup>[11]</sup>,这可能是由于冠状动脉顺行血流与肌桥前端逆行血流相互碰撞,引起血流振荡和逆转,影响近端壁剪切应力(wall shear stress, WSS)、机械应力<sup>[4,8,12]</sup>。WSS是指由于血液流动而施加于血管壁上的切向力。低WSS已被证明与内皮功能障碍和动脉粥样硬化的发展有关<sup>[13-14]</sup>。除WSS外,其他血流动力学因素血流循环和血液峰值停留时间,可能影响动脉斑块的起始和进展<sup>[15-16]</sup>。因此,了解生物力学因素对心肌桥近端冠状动脉血流及斑块形成的影响具有重要的临床意义。

对于心肌桥患者,只有少数研究使用简化的体内和体外模型来获得剪切应力,表明心肌桥内和近端的WSS

异常,这可能与近端易形成动脉粥样硬化相关。然而这些大多为理论推导性研究<sup>[17-18]</sup>。SHARZEHEE等<sup>[19]</sup>通过数值和实验方法证明,与类似的狭窄病变(虚拟产生)相比,心肌桥患者的压降明显更低。NIKOLICY等<sup>[18]</sup>使用理想的2D模型比较心肌桥入口和出口生物力学环境的差异。这些研究都没有使用基于3D的患者特异性模型,无法全面评估心肌桥近端斑块生长相关的力学环境。基于CCTA的无创计算流体力学分析可以实现壁压力、管壁形变、流速、流线和壁切应力等多参数力学测量<sup>[20-22]</sup>。但大多数斑块在不同时间点表现出不同空间上生长的异质性,肉眼常常无法识别。通过组学方法高通量地提取血流动力学的多样性特征,可能可以更早期、精准分析斑块发生发展不同时间生物力学环境的变化,提示与心肌桥近端斑块形成相关的生物力学特征。因此,本研究的主要目的是分析基于CCTA的力学组学对心肌桥近端斑块形成的预测价值。

## 1 资料与方法

### 1.1 纳入人群

回顾性搜集东部战区总医院自2007年1月1日-2021年4月31日行CCTA检查示左冠状动脉前降支心肌桥的患者,本研究已经过东部战区总医院医学伦理委员会批准(意见号:2023DZKY-124-01),所有患者免除知情同意。斑块形成定义为随访CCTA时左冠状动脉前降支近

段任意位置、任何性质的斑块,若同一患者行两次以上 CCTA 检查,以第一次出现斑块时为终点,记录随访时间及基线时患者的临床特征,包括年龄、性别、高血压、高血脂、糖尿病和吸烟。对纳入人群按照年龄、性别进行 1:1 匹配分为斑块形成组和无斑块形成组。

### 1.2 CCTA 扫描及解剖学参数测量

所有扫描均使用德国 Siemens 公司第一、二代双源 CT (SOMATOM Definition Flash, Siemens Healthineers, Forchheim, Germany)。第一代双源 CT 采用回顾性心电图门控技术,自动获取最佳收缩及舒张期图像。第二代双源 CT 采用前瞻性心电图门控技术,在 30%~80% R-R 间期内进行扫描<sup>[23]</sup>,以 30%~35% 和 66%~75% 期相重建,重建间隔为 0.5 mm,层厚为 0.75 mm。扫描参数为:管电压 100 或 120 kVp;重建层厚 0.75 mm;重建间隔 0.5 mm。所有数据导入专用的工作站 (Syngo Via, 西门子) 进行分析测量,首先由两名经验丰富的影像科医生对图像质量进行评分,1=无法诊断;2=可以接受;3=良好;4=极佳,1 分的图像被排除在外。采用舒张期测量心肌桥的长度、深度、位置,采用双期图像测量狭窄程度以及壁冠状动脉收缩期狭窄指数。根据深度将心肌桥分为表浅型 ( $\leq 2$  mm) 和纵深型 ( $> 2$  mm),根据长度分为长心肌桥 ( $> 3.0$  cm) 和短心肌桥 ( $\leq 3.0$  cm)<sup>[24]</sup>。随访 CCTA 终点的确定由两名影像科医生 (分别具有 2 年和 6 年的 CCTA 工作经验) 进行确定。

### 1.3 力学组学提取

使用 Aladdin Solutions CCTA 分析平台 (南京景三医疗科技有限公司),对 CCTA 图像进行分割并将选定的感兴趣区域的 mask 重建得到 3D 模型,作为计算流体动力学分析的几何模型。首先是网格生成:将 mask 文件转化成 stl 格式网格文件,利用拉普拉斯平滑算法进行网格平滑;将光滑后的网格利用 delaunay 算法进行实体网格填充。网格填充算法通过调用 VMTK 工具进行。表面网格、内部网格、边界层大小分别为 100  $\mu\text{m}$ 、500  $\mu\text{m}$ 、100  $\mu\text{m}$ ,边界层增长率 1.1<sup>[25]</sup>,然后进行流体动力学分析,假设血液是不可压有黏的牛顿流体,血液密度和黏度为 1.06  $\text{g}/\text{cm}^3$  和 0.0035 Pa,最后 Lagrangian-Eulerian 方法求解流体动力学控制方程,得到相关血液动力学参数<sup>[26]</sup>,包括:最大和最小切应力、基于时间平均切应力 (time-averaged WSS, TAWSS)、切应力梯度 (WSS gradient, WSSG)、振荡剪切系数 (oscillatory shear index, OSI)、粒子相对滞留时间 (relative residence time, RRT)、血流速度和压力分布等。提取的感兴趣区域为左冠状动脉前降支近段 (左主干分叉处至心肌桥入口处)。各主要参数通过如下方程得到:

TAP: 一个心动周期内单位面积管壁平均压力;

$$\text{TAP} = \frac{1}{T_c} \int_0^{T_c} p dt$$

TAWSS: 一个心动周期内管壁剪切应力平均值;

$$\text{TAWSS} = \frac{1}{T_c} \int_0^{T_c} |\tau_w| dt$$

OSI: 震荡剪切因数,一个心动周期内管壁剪切应力方向幅度变化程度量化指标;

$$\text{OSI} = \frac{1}{2} \left( 1 - \frac{\left| \int_0^{T_c} \tau_w dt \right|}{\int_0^{T_c} |\tau_w| dt} \right)$$

RRT: 相对停留时间,量化血流在对应壁面附近停留时间;

$$\text{RRT} = [(1 - 2 \times \text{OSI}) \times \text{TAWSS}]^{-1}$$

其中  $p$  是压力,  $T_c$  是心动周期时长,  $\tau_w$  是瞬时管壁剪切应力,  $t$  是时间<sup>[27]</sup>。所有参数抽取在 Aladdin Solutions CCTA 分析平台中进行。

### 1.4 机器学习模型构建

匹配后的数据按 7:3 比例被随机分为训练集和验证集,并在两个数据集中保持阳性比例一致。为了减少特征冗余以及避免潜在的过拟合,本研究进行了特征筛选。随机森林是一种通常不需要太多调整参数就可以实现较好性能的算法, Boruta 是一种基于随机森林的算法,先生成影子特征,再不断迭代循环比较原始特征和影子特征的重要性,通过迭代的方式逐步消除无关特征,从而实现特征筛选,产生与斑块形成最相关的特征的排序并给出特征重要性的数值估计<sup>[28]</sup>。选择特征的过程中进行超参数调整构建模型,选择最重要的特征与最合适的参数,同时采用 resampling 的技术来构建最优随机森林模型。最后,利用随机森林,基于力学组学特征,为每例患者发生事件的概率大小进行赋值评分。

### 1.5 统计学方法

使用 SPSS 26.0 版本 (SPSS, IL) 和 MedCalc 版本 19.0.7 (MedCalc 软件) 对数据进行统计学分析。使用 Kolmogorov-Smirnov 检验定量数据是否符合正态分布,符合正态分布的连续性变量以  $\bar{x} \pm s$  表示,组间对比采用单因素方差分析,不符合正态分布则采用四分位间距 ( $P_{25} \sim P_{75}$ ) 表示,组间对比采用 Mann-Whitney  $U$  检验,分类变量以数字和百分比表示,组间对比采用卡方检验。根据年龄和性别按照 1:1 匹配斑块形成 (阳性) 组和无斑块形成 (阴性) 组。利用多因素 Cox 回归模型计算危险比 (hazard ratio, HR) 并记录 95% 置信区间 (confidence interval, CI)。通过向前-有条件的逐级选择筛选临床、解剖参数。使用对数秩检验和 Kaplan-Meier 曲线图比较各

组间的累积斑块形成率。利用受试者工作特征曲线的曲线下面积(area under the curve, AUC), 对力学组学模型进行评估, 并采用Delong检验进行比较<sup>[29]</sup>。除AUC外, 本研究还计算了敏感性、特异性, 并报告了95%CI。P<0.05为差异有统计学意义。

## 2 结果

### 2.1 临床和解剖特征

本研究共收集192例本院数据, 其中52例患者在随访时CCTA显示有斑块生成, 按年龄性别匹配后共纳入104例行重复CCTA检查的心肌桥患者。患者基线特征见

表1。随访时间中位数为3.0年, 其中随访时有斑块和无斑块生成各有52例, 按心肌桥分类, 表浅型心肌桥占83.65%(87/104), 纵深型心肌桥占16.35%(17/104); 长心肌桥占35.58%(37/104), 短心肌桥占64.42%(67/104)。总人群的平均年龄为(54.56±10.56)岁, 斑块形成组为(53.70±10.24)岁, 无斑块形成组为(55.41±10.90)岁; 总人群中75.00%(78/104)为男性, 斑块形成组男性占76.92%(40/52), 无斑块形成组男性比例为73.08%(38/52)。斑块形成组与非斑块形成组间有差异的临床因素为吸烟史(21.15% vs. 5.77%, P=0.04), 其余的临床及解剖学特征差异无统计学意义(P>0.05)。

表1 患者基线特征

Table 1 Patient baseline characteristics

Item	All patients (n=104)	Plaque formation (n=52)	No plaque formation (n=52)	P
Age/yr.	54.56±10.56	53.70±10.24	55.41±10.90	0.41
Male/case (%)	78 (75.00)	40 (76.92)	38 (73.08)	0.43
Diabetes/case (%)	26 (25.00)	10 (19.23)	16 (30.77)	0.26
Hypertension/case (%)	47 (45.19)	21 (40.38)	26 (50.00)	0.43
Smoking/case (%)	14 (13.46)	11 (21.15)	3 (5.77)	0.04
Hypercholesterolemia/case (%)	29 (27.88)	14 (26.92)	15 (28.85)	>0.99
MB location/mm, median (P <sub>25</sub> -P <sub>75</sub> )	36.90 (28.00-48.47)	37.15 (27.05-52.20)	36.90 (31.23-45.87)	0.89
MB length/mm, median (P <sub>25</sub> -P <sub>75</sub> )	24.40 (16.27-34.32)	25.10 (17.60-35.72)	23.60 (14.92-32.47)	0.44
MB depth/mm, median (P <sub>25</sub> -P <sub>75</sub> )	1.00 (0.00-1.72)	0.95 (0.00-1.52)	1.05 (0.00-2.00)	0.41
MB stenosis/%	20.99±11.46	21.42±13.28	20.56±9.40	0.70
Minimal systolic diameter/mm, median (P <sub>25</sub> -P <sub>75</sub> )	1.75 (1.50-2.00)	1.80 (1.50-1.92)	1.70 (1.48-2.00)	0.46
Minimal diastolic diameter/mm, median (P <sub>25</sub> -P <sub>75</sub> )	2.00 (1.80-2.20)	2.00 (1.80-2.20)	1.90 (1.80-2.22)	0.91
Systolic compression index (median [P <sub>25</sub> -P <sub>75</sub> ])	0.11 (0.08-0.17)	0.11 (0.07-0.17)	0.13 (0.08-0.18)	0.31

MB: myocardial bridging.

### 2.2 力学组学参数提取及模型建立

基于心肌桥患者基线CCTA共提取左冠状动脉前降支近端力学参数1698个, 104例入组心肌桥患者按照7:3分为训练集(n=74)和验证集(n=30)。经随机森林算法提取出7个参数构建最优模型并在验证集中进行验证, 各参数特征重要性排序及每例患者模型预测的柱状图见图1, 其中压力相关参数有6个, 而壁剪切应力相关参数仅有1个, 呈正相关, 特征重要性为0.03。特征重要性最高的是TimeSTDPressure\_Median, 即标准偏差时间上的压力的中位数, 权重系数为0.04。力学组学模型在全部人群、训练集和验证集的敏感性、准确性分别为0.87(0.74~0.94)、0.73(0.59~0.84)、0.86(0.71~0.96)、

0.78(0.62~0.90)、0.99(0.78~1.00)、0.53(0.27~0.79)。

### 2.3 力学组学模型对斑块形成预测能力

根据组间比较的结果(表1), 将每例患者的力学组学赋值评分和是否吸烟纳入多因素Cox回归模型中, 力学组学(HR=10.58; 95%CI: 3.23~34.64, P≤0.001)与斑块形成呈正相关, 而吸烟(HR=0.74; 95%CI: 0.26~2.16, P=0.58)与斑块形成无关。如图2所示, 对斑块形成的累积事件发生率进行了对数秩检验, 生成了Kaplan-Meier生存曲线, 结果显示力学组学赋分较高组(≥0.46)能显著对心肌桥患者有无斑块生成进行危险分层(P<0.001)。图3显示了整体水平(A)、训练集(B)、验证集(C)、表浅心肌桥组(D)、纵深心肌桥组(E)、短心肌桥组(F)和长心肌桥组

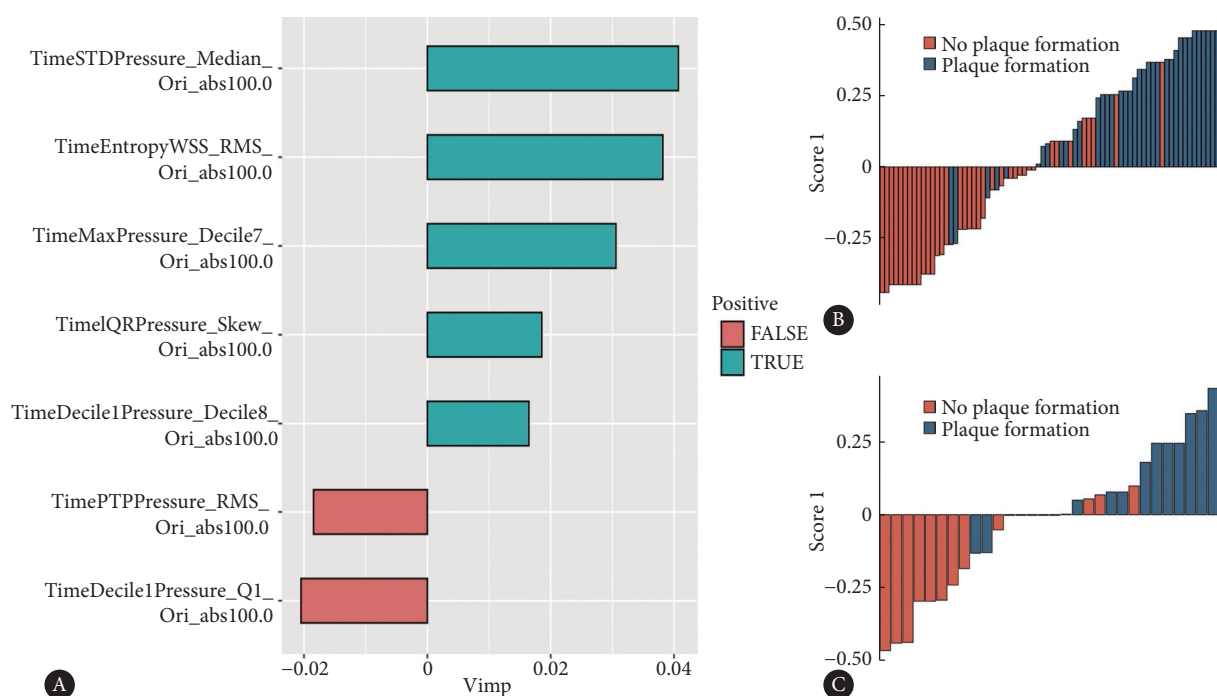


图 1 所选特征权重排序及每例患者模型预测的柱状图

Fig 1 Histogram of the weight ranking of selected features and the model predictions for each patient

A, Feature weight ranking of the mechanics model; B, predictions of the model for the training set; C, predictions of the model for the validation set.

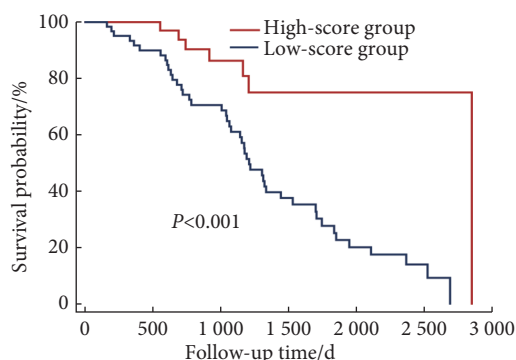


图 2 总人群Kaplan-Meier生存曲线

Fig 2 Kaplan-Meier survival curves in the general patient population

High-score group ( $n=61$ ), low-score group ( $n=43$ ).

(G) 力学组学预测斑块形成的受试者工作特征曲线和 AUC, 其 AUC 分别为 0.88 (0.82 ~ 0.95)、0.89 (0.82 ~ 0.96)、0.86 (0.74 ~ 0.99)、0.92 (0.86 ~ 0.97)、0.69 (0.42 ~ 0.96)、0.91 (0.83 ~ 0.98) 和 0.86 (0.74 ~ 0.98)。除纵深心肌桥组外, 力学组学模型在各组内对斑块形成都有较好的预测能力 (所有  $P < 0.001$ )。

### 3 讨论

左冠状动脉前降支中段心肌桥的存在是其近端冠状动脉粥样硬化的独立危险因素<sup>[11]</sup>, 既往血管内超声及理论研究表明血流动力学的改变可能导致肌桥近端动脉粥

样硬化斑块的形成, 而在壁冠状动脉段内不容易形成斑块<sup>[30]</sup>。随着影像技术的更新及机器学习的发展, 基于 CCTA 计算流体力学组学的方法可以对心肌桥患者进行无创功能评估, 因此本研究采用基于 CCTA 的计算流体力学的方法提取心肌桥近端力学组学参数, 结果表明基于不同时间节点提取的力学参数对斑块形成有着较高的预测价值, 有望成为预测斑块形成的新工具。

心肌桥由于动态收缩的特性, 导致心肌桥入口处血流紊乱, 而众多研究表明紊乱的血流动力学可以导致管壁内皮细胞受损, 进一步导致血管活性物质的增加, 如内皮一氧化氮合酶、内皮素-1 和血管紧张素转换酶, 致使心肌桥入口前 2 ~ 3 cm 容易出现动脉粥样硬化<sup>[31]</sup>。因此, 本研究选取心肌桥患者作为研究斑块形成相关血流动力学的活体模型。之前研究表明基于计算流体力学的冠状动脉血流储备分数 (fractional flow reserve based on coronary computed tomography angiography, CT-FFR) 是心肌桥近端斑块形成的独立预测因子且优于临床和解剖参数<sup>[32]</sup>。总体上, 针对心肌桥患者的血流动力学研究较少, 目前有关血流动力学和动脉粥样硬化的研究大都基于血管内超声和冠状动脉造影 (invasive coronary angiography, ICA) 的计算流体力学模型, 但这些技术都是有创技术, 难以在临床推广应用。少数基于 CCTA 的研究证实心肌桥近端 WSS 较低, 而壁冠状动脉内 WSS 较高<sup>[29, 33-34]</sup>。本研究同时

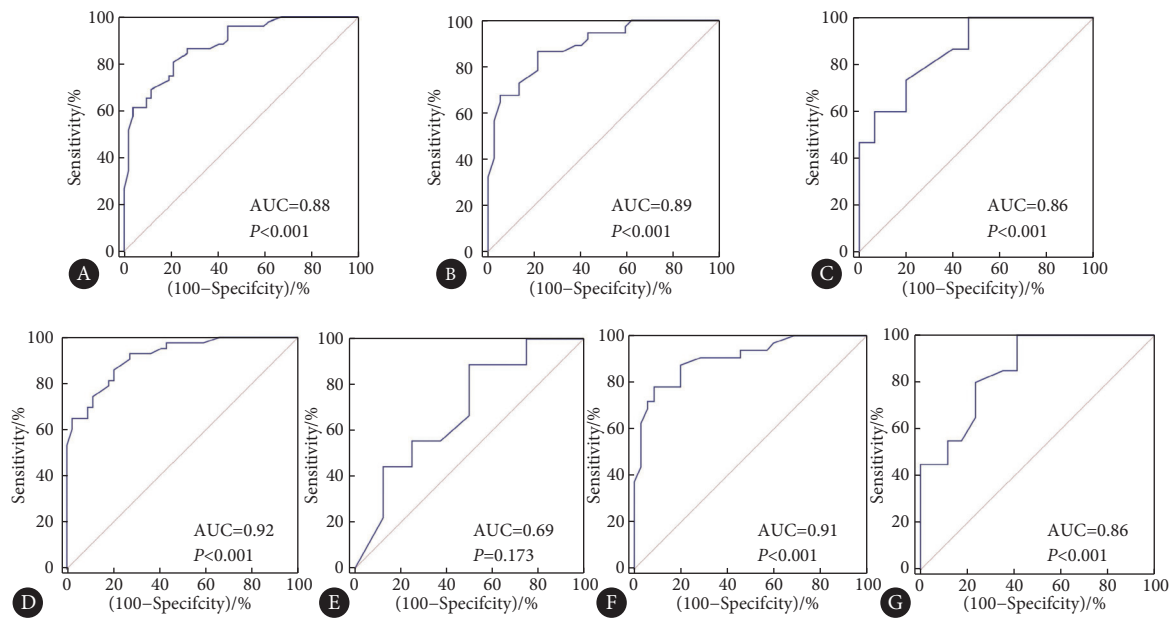


图3 力学组学模型预测斑块形成的受试者工作特征曲线图

Fig 3 ROC curves for the prediction of plaque formation using mechanics modeling

A, All patients ( $n=104$ ); B, the training set ( $n=74$ ); C, the validation set ( $n=30$ ); D, superficial myocardial bridge group ( $n=87$ ); E, deep myocardial bridge group ( $n=17$ ); F, short myocardial bridge group ( $n=67$ ); G, long myocardial bridge group ( $n=37$ ).

提取了时间相关参数RRT、压力相关参数TAP、流体力学相关参数TAWSS和WSS等及其一阶统计参数,首次使用新的计算建模技术,模拟动态血管壁压缩,多维度无创评估人类病例中生物力学因素和斑块形成之间的相互关系。

除生物力学因素外,心肌桥形态学与血流动力学密切相关,人们认为较长和较深的心肌桥因其较严重的收缩可能导致近端更多的内皮损伤和严重的动脉粥样硬化<sup>[35]</sup>。JAVADZADEGAN等<sup>[36]</sup>的研究证实与没有心肌桥相比,有心肌桥的患者在左冠状动脉近端节段斑块负荷更重且心肌桥长度的增加与WSS的减少和RRT的增加有关。本研究在按照年龄性别匹配、组间对比后只有吸烟史在斑块有无形成组之间差异有统计学意义且在后续的回归分析中被排除在外,表明本研究较好地平衡了两组间的混杂因素且力学组学因素优于其他传统心血管危险因素和心肌桥解剖学因素。力学组学模型在表浅、长、短心肌桥组内,对近端斑块形成都表现出了良好的预测性能,纵深型心肌桥患者仅占16%,数量较少,这可能是没有表现出统计学差异的原因之一。

本研究创新点在于从生物力学环境多样性的角度,阐明动脉粥样硬化发生的力学机制,在研究理念上有较强的创新性,为冠心病的早期预警及防治提供新的思路。此外,基于无创CCTA计算流体力学组学的方法,对血流动力学多样性参数提取,为影像无创评估冠状动脉功能学提供新手段。本研究尚存在一定局限性。首先,只纳入了位于左冠状动脉前降支的心肌桥,虽然这是最

常见的位置。其次,本研究为单中心回顾性研究,样本量小且缺乏外部验证数据,需要进行更大规模的研究来评估。第三,考虑到时间成本和软件目前存在的限制,本研究的CFD模型没有考虑侧枝的影响,这可能会对结果产生一定的影响,今后将不断对模型进行优化以缩短计算时间和分析侧枝可能产生的作用。最后,没有考虑到心脏运动的影响。然而,已有研究表明,心脏运动对冠状动脉血流动力学的影响可以忽略不计<sup>[37]</sup>。

总之,本研究基于CCTA和机器学习表明力学组学对于心肌桥前端斑块形成具有较好的预测价值,对斑块发生的病理机制及其早期防治提供新的见解,但需进一步大样本和外部验证数据的支持。

\* \* \*

**作者贡献声明** 陈艳春负责调查研究、研究方法、验证和初稿写作,郑金负责数据审编、正式分析和可视化,滕忠照负责研究项目管理、软件、监督指导和审读与编辑写作,张龙江负责论文构思、提供资源、监督指导和审读与编辑写作。所有作者已经同意将文章提交给本刊,且对将要发表的版本进行最终定稿,并同意对工作的所有方面负责。

**Author Contribution** CHEN Yanchun is responsible for investigation, methodology, validation, and writing--original draft. ZHENG Jin is responsible for data curation, formal analysis, and visualization. TENG Zhongzhao is responsible for project administration, software, supervision, and writing--review and editing. ZHANG Longjiang is responsible for conceptualization, resources, supervision, and writing--review and editing. All authors consented to the submission of the article to the Journal. All authors approved the final version to be published and agreed to take responsibility for all aspects of the work.

**利益冲突** 本文作者滕忠照为南京景三医疗科技有限公司法定代表人, Aladdin Solutions CCTA软件由该公司免费提供。除此之外, 所有作者均声明不存在利益冲突。

**Declaration of Conflicting Interests** TENG Zhongzhao is the legal representative of Nanjing Jingsan Medical Science and Technology, Ltd. Aladdin Solutions CCTA, a computer program, was provided free of charge by the company. Apart from these, all authors declare that there are no competing interests.

### 参 考 文 献

- [1] THYGESEN K, ALPERT J S, WHITE H D. Joint ESC/ACCF/AHA/WHF Task Force for the redefinition of myocardial infarction. Universal definition of myocardial infarction. *J Am Coll Cardiol*, 2007, 50(22): 2173-2195. doi: [10.1016/j.jacc.2007.09.011](https://doi.org/10.1016/j.jacc.2007.09.011).
- [2] NEREM R M. Vascular fluid mechanics, the arterial wall, and atherosclerosis. *J Biomech Eng*, 1992, 114(3): 274-282. doi: [10.1115/1.2891384](https://doi.org/10.1115/1.2891384).
- [3] HERRINGTON W, LACEY B, SHERLIKER P, *et al*. Epidemiology of atherosclerosis and the potential to reduce the global burden of atherothrombotic disease. *Circ Res*, 2016, 118(4): 535-546. doi: [10.1161/CIRCRESAHA.115.307611](https://doi.org/10.1161/CIRCRESAHA.115.307611).
- [4] CORBAN M T, HUNG O Y, ESHTEHARDI P, *et al*. Myocardial bridging: contemporary understanding of pathophysiology with implications for diagnostic and therapeutic strategies. *J Am Coll Cardiol*, 2014, 63(22): 2346-2355. doi: [10.1016/j.jacc.2014.01.049](https://doi.org/10.1016/j.jacc.2014.01.049).
- [5] TARANTINI G, MIGLIORE F, CADEMARTIRI F, *et al*. Left anterior descending artery myocardial bridging: a clinical approach. *J Am Coll Cardiol*, 2016, 68(25): 2887-2899. doi: [10.1016/j.jacc.2016.09.973](https://doi.org/10.1016/j.jacc.2016.09.973).
- [6] La GRUTTA L, RUNZA G, Lo RE G, *et al*. Prevalence of myocardial bridging and correlation with coronary atherosclerosis studied with 64-slice CT coronary angiography. *Radiol Med*, 2009, 114(7): 1024-1036. doi: [10.1007/s11547-009-0446-y](https://doi.org/10.1007/s11547-009-0446-y).
- [7] ALEGRIA J R, HERRMANN J, HOLMES D R, Jr, *et al*. Myocardial bridging. *Eur Heart J*, 2005, 26(12): 1159-1168. doi: [10.1093/eurheartj/ehi203](https://doi.org/10.1093/eurheartj/ehi203).
- [8] BOURASSA M G, BUTNARU A, LESPÉRANCE J, *et al*. Symptomatic myocardial bridges: overview of ischemic mechanisms and current diagnostic and treatment strategies. *J Am Coll Cardiol*, 2003, 41(3): 351-359. doi: [10.1016/s0735-1097\(02\)02768-7](https://doi.org/10.1016/s0735-1097(02)02768-7).
- [9] DESSEIGNE P, TABIB A, LOIRE R. Myocardial bridging on the left anterior descending coronary artery and sudden death. Apropos of 19 cases with autopsy. *Arch Mal Coeur Vaiss*, 1991, 84(4): 511-516.
- [10] FELD H, GUADANINO V, HOLLANDER G, *et al*. Exercise-induced ventricular tachycardia in association with a myocardial bridge. *Chest*, 1991, 99(5): 1295-1296. doi: [10.1378/chest.99.5.1295](https://doi.org/10.1378/chest.99.5.1295).
- [11] NAKAURA T, NAGAYOSHI Y, AWAI K, *et al*. Myocardial bridging is associated with coronary atherosclerosis in the segment proximal to the site of bridging. *J Cardiol*, 2014, 63(2): 134-139. doi: [10.1016/j.jcc.2013.07.005](https://doi.org/10.1016/j.jcc.2013.07.005).
- [12] HERRMANN J, HIGANO S T, LENON R J, *et al*. Myocardial bridging is associated with alteration in coronary vasoreactivity. *Eur Heart J*, 2004, 25(23): 2134-2142. doi: [10.1016/j.ehj.2004.08.015](https://doi.org/10.1016/j.ehj.2004.08.015).
- [13] WEBER C, NOELS H. Atherosclerosis: current pathogenesis and therapeutic options. *Nat Med*, 2011, 17(11): 1410-1422. doi: [10.1038/nm.2538](https://doi.org/10.1038/nm.2538).
- [14] MALEK A M, ALPER S L, IZUMO S. Hemodynamic shear stress and its role in atherosclerosis. *JAMA*, 1999, 282(21): 2035-2042. doi: [10.1001/jama.282.21.2035](https://doi.org/10.1001/jama.282.21.2035).
- [15] CHENG C, TEMPEL D, Van HAPEREN R, *et al*. Atherosclerotic lesion size and vulnerability are determined by patterns of fluid shear stress. *Circulation*, 2006, 113(23): 2744-2753. doi: [10.1161/CIRCULATIONAHA.105.590018](https://doi.org/10.1161/CIRCULATIONAHA.105.590018).
- [16] JAVADZADEGAN A, YONG A S, CHANG M, *et al*. Flow recirculation zone length and shear rate are differentially affected by stenosis severity in human coronary arteries. *Am J Physiol Heart Circ Physiol*, 2013, 304(4): H559-H566. doi: [10.1152/ajpheart.00428.2012](https://doi.org/10.1152/ajpheart.00428.2012).
- [17] DORIOT P A, DORSAZ P A, NOBLE J. Could increased axial wall stress be responsible for the development of atheroma in the proximal segment of myocardial bridges? *Theor Biol Med Model*, 2007, 4: 29. doi: [10.1186/1742-4682-4-29](https://doi.org/10.1186/1742-4682-4-29).
- [18] NIKOLIĆ D, RADOVIĆ M, ALEKSANDRIĆ S, *et al*. Prediction of coronary plaque location on arteries having myocardial bridge, using finite element models. *Comput Methods Programs Biomed*, 2014, 117(2): 137-144. doi: [10.1016/j.cmpb.2014.07.012](https://doi.org/10.1016/j.cmpb.2014.07.012).
- [19] SHARZEHEE M, SEDDIGHI Y, SPRAGUE E A, *et al*. A hemodynamic comparison of myocardial bridging and coronary atherosclerotic stenosis: a computational model with experimental evaluation. *J Biomech Eng*, 2021, 143(3): 031013. doi: [10.1115/1.4049221](https://doi.org/10.1115/1.4049221).
- [20] HAN D, STARIKOV A, Ó HARTAIGH B, *et al*. Relationship between endothelial wall shear stress and high-risk atherosclerotic plaque characteristics for identification of coronary lesions that cause ischemia: a direct comparison with fractional flow reserve. *J Am Heart Assoc*, 2016, 5(12): e004186. doi: [10.1161/JAHA.116.004186](https://doi.org/10.1161/JAHA.116.004186).
- [21] PARK J B, CHOI G, CHUN E J, *et al*. Computational fluid dynamic measures of wall shear stress are related to coronary lesion characteristics. *Heart*, 2016, 102(20): 1655-1661. doi: [10.1136/heartjnl-2016-309299](https://doi.org/10.1136/heartjnl-2016-309299).
- [22] LEE J M, CHOI G, KOO B K, *et al*. Identification of high-risk plaques destined to cause acute coronary syndrome using coronary computed tomographic angiography and computational fluid dynamics. *JACC Cardiovasc Imaging*, 2019, 12(6): 1032-1043. doi: [10.1016/j.jcmg.2018.01.023](https://doi.org/10.1016/j.jcmg.2018.01.023).
- [23] LIU S H, YANG Q, CHEN J H, *et al*. Myocardial bridging on dual-source computed tomography: degree of systolic compression of mural coronary artery correlating with length and depth of the myocardial bridge. *Clin*

- Imaging, 2010, 34(2): 83-88. doi: [10.1016/j.clinimag.2009.05.010](https://doi.org/10.1016/j.clinimag.2009.05.010).
- [24] ZHOU F, WANG Y N, SCHOEPP U J, *et al.* Diagnostic performance of machine learning based ct-ffr in detecting ischemia in myocardial bridging and concomitant proximal atherosclerotic disease. *Can J Cardiol*, 2019, 35(11): 1523-1533. doi: [10.1016/j.cjca.2019.08.026](https://doi.org/10.1016/j.cjca.2019.08.026).
- [25] SHI Y, ZHENG J, ZHANG Y, *et al.* The influence of flow distribution strategy for the quantification of pressure- and wall shear stress-derived parameters in the coronary artery: A CTA-based computational fluid dynamics analysis. *J Biomech*, 2023, 161: 111857. doi: [10.1016/j.jbiomech.2023.111857](https://doi.org/10.1016/j.jbiomech.2023.111857).
- [26] TENG Z, YUAN J, FENG J, *et al.* The influence of constitutive law choice used to characterise atherosclerotic tissue material properties on computing stress values in human carotid plaques. *J Biomech*, 2015, 48(14): 3912-3921. doi: [10.1016/j.jbiomech.2015.09.023](https://doi.org/10.1016/j.jbiomech.2015.09.023).
- [27] LOPES D, PUGA H, TEIXEIRA J, *et al.* Blood flow simulations in patient-specific geometries of the carotid artery: a systematic review. *J Biomech*, 2020, 111: 110019. doi: [10.1016/j.jbiomech.2020.110019](https://doi.org/10.1016/j.jbiomech.2020.110019).
- [28] QUER G, ARNAOUT R, HENNE M, *et al.* Machine learning and the future of cardiovascular care: JACC State-of-the-Art review. *J Am Coll Cardiol*, 2021, 77(3): 300-313. doi: [10.1016/j.jacc.2020.11.030](https://doi.org/10.1016/j.jacc.2020.11.030).
- [29] DeLONG E R, DeLONG D M, CLARKE-PEARSON D L. Comparing the areas under two or more correlated receiver operating characteristic curves: a nonparametric approach. *Biometrics*, 1988, 44(3): 837-845. doi: [10.2307/2531595](https://doi.org/10.2307/2531595).
- [30] JAVADZADEGAN A, MOSHFEGH A, HASSANZADEH AFROUZI H. Relationship between myocardial bridge compression severity and haemodynamic perturbations. *Comput Methods Biomech Biomed Engin*, 2019, 22(7): 752-763. doi: [10.1080/10255842.2019.1589458](https://doi.org/10.1080/10255842.2019.1589458).
- [31] KHAN M O, NISHI T, IMURA S, *et al.* Colocalization of coronary plaque with wall shear stress in myocardial bridge patients. *Cardiovasc Eng Technol*, 2022, 13(5): 797-807. doi: [10.1007/s13239-022-00616-4](https://doi.org/10.1007/s13239-022-00616-4).
- [32] ZHOU F, TANG C X, SCHOEPP U J, *et al.* Machine learning using CT-FFR predicts proximal atherosclerotic plaque formation associated With LAD myocardial bridging. *JACC Cardiovasc Imaging*, 2019, 12(8 Pt 1): 1591-1593. doi: [10.1016/j.jcmg.2019.01.018](https://doi.org/10.1016/j.jcmg.2019.01.018).
- [33] Van Den HOOGEN I J, SCHULTZ J, KUNEMAN J H, *et al.* Detailed behaviour of endothelial wall shear stress across coronary lesions from non-invasive imaging with coronary computed tomography angiography. *Eur Heart J Cardiovasc Imaging*, 2022, 23(12): 1708-1716. doi: [10.1093/ehjci/jeac095](https://doi.org/10.1093/ehjci/jeac095).
- [34] STERNHEIM D, POWER D A, SAMTANI R, *et al.* Myocardial bridging: Diagnosis, functional assessment, and management: JACC State-of-the-Art Review. *J Am Coll Cardiol*, 2021, 78(22): 2196-2212. doi: [10.1016/j.jacc.2021.09.859](https://doi.org/10.1016/j.jacc.2021.09.859).
- [35] AYDIN A, ÇUBUK R, ATASOY M M, *et al.* The morphologic and functional features of LAD myocardial bridging at multi-detector computed tomography coronary angiography: correlation with coronary artery disease. *Turk Kardiyol Dern Ars*, 2015, 43(1): 31-37. doi: [10.5543/tkda.2015.23672](https://doi.org/10.5543/tkda.2015.23672).
- [36] JAVADZADEGAN A, MOSHFEGH A, MOHAMMADI M, *et al.* Haemodynamic impacts of myocardial bridge length: a congenital heart disease. *Comput Methods Programs Biomed*, 2019, 175: 25-33. doi: [10.1016/j.cmpb.2019.03.017](https://doi.org/10.1016/j.cmpb.2019.03.017).
- [37] KABINEJADIAN F, GHISTA D N. Compliant model of a coupled sequential coronary arterial bypass graft: effects of vessel wall elasticity and non-Newtonian rheology on blood flow regime and hemodynamic parameters distribution. *Med Eng Phys*, 2012, 34(7): 860-872. doi: [10.1016/j.medengphy.2011.10.001](https://doi.org/10.1016/j.medengphy.2011.10.001).

(2024 - 08 - 14收稿, 2024 - 10 - 24修回)

编辑 汤洁



**开放获取** 本文使用遵循知识共享署名—非商业性使用4.0国际许可协议 (CC BY-NC 4.0), 详细信息请访问

<https://creativecommons.org/licenses/by/4.0/>。

**OPEN ACCESS** This article is licensed for use under Creative Commons Attribution-NonCommercial 4.0 International license (CC BY-NC 4.0). For more information, visit <https://creativecommons.org/licenses/by/4.0/>.

© 2024 《四川大学学报(医学版)》编辑部

Editorial Office of *Journal of Sichuan University (Medical Sciences)*